doi:10.1246/cl.2011.822
Published on the web July 2, 2011

Synthesis and n-Type Field-effect Transistor Characteristics of Dioxopyrrolopyrrole Derivatives

Yuki Suna,[1] Jun-ichi Nishida,[1] Yoshihide Fujisaki,[2] and Yoshiro Yamashita*[1]
[1]*Department of Electronic Chemistry, Interdisciplinary Graduate School of Science and Engineering, Tokyo Institute of Technology, G1-8, 4259 Nagatsuta, Midori-ku, Yokohama, Kanagawa 225-8502*
[2]*NHK Science and Technical Research Laboratories, Kinuta, Setagaya-ku, Tokyo 157-8510*

(Received May 20, 2011; CL-110427; E-mail: yoshiro@echem.titech.ac.jp)

Dioxopyrrolopyrrole derivatives with electron-withdrawing groups have been synthesized and applied to organic field-effect transistors as n-channel semiconductors. A derivative with an intermolecular hydrogen-bonding network showed a good electron mobility up to $2.9 \times 10^{-2}\,cm^2\,V^{-1}\,s^{-1}$.

n-Type organic semiconductors for organic field-effect transistors (OFETs) have attracted considerable attention for the fabrication of complementary logic circuits.[1] However, the development of high-performance ambient-stable n-type materials has lagged behind that of p-type materials due to the inherent instability of organic anions toward oxygen and water.

Dioxopyrrolopyrrole (DPP) consisting of a fused heterocycle possesses a planar π-electron core and two amide groups. DPP derivatives have been used as high-performance organic pigments with brilliant red color.[2] Recently, DPP-based small molecules have been attracting much attention as materials for organic electronics because of their promising charge transporting performance in solar cells as well as OFETs.[3,4] The formation of multiple hydrogen-bonding networks between the amide groups is a particularly noteworthy characteristic of DPP. This strong intermolecular interaction makes DPPs into environmentally stable pigments which can be widely used in industry. This is also attractive for high-performance n-type materials because a close-packed crystal structure with hydrogen bonding enhances electron hopping between the molecules.[5] Although only one DPP-based small molecule with a hydrogen-bonding network was reported to show FET characteristics, it shows p-type behavior with moderate mobility of 1.43×10^{-5} $cm^2\,V^{-1}\,s^{-1}$.[4b]

We report here the first examples of n-type semiconducting small molecular DPP derivatives. We introduced trifluoromethylphenyl (CF_3Ph) groups onto the DPP core. The CF_3Ph group is expected to provide DPP with a low-lying LUMO level suitable for electron transport.[6] We have also investigated the effects of the hydrogen-bonding network between the DPP molecules on the semiconducting properties.

DPP derivatives possessing CF_3Ph groups and hydrogen-bonding sites were synthesized as shown in Scheme 1. For comparison, *N*-methyl-substituted DPP derivatives that cannot form intermolecular hydrogen-bonding networks were also synthesized. IR spectroscopy (Figure S1[9]) confirmed the formation of N–H···O hydrogen bonding between the amide hydrogen atoms and the carbonyl oxygen atoms. In the spectra of *N*-methyl derivatives **2** and **4**, the free-carbonyl stretching vibration was observed at 1670 and 1661 cm^{-1}, respectively. These bands shift to 1640 and 1634 cm^{-1} in **1** and **3**, respectively, where multiple peaks assigned to the hydrogen-bonded N–H are observed within the range of 2700 to 3200 cm^{-1}. In the hydrogen-bonded DPP crystals, π–π interactions exist along the stacking direction of molecules and four intermolecular hydrogen bonds per molecule between the NH group of one molecule and the oxygen atom of the neighboring one horizontally extend to the molecular plane. Although the single crystals of **1** and **3** could not be obtained, such a hydrogen-bonding network is commonly observed in DPP crystals and contributes to the large red-shifts in the spectra of DPP solids compared with those in solution.[7]

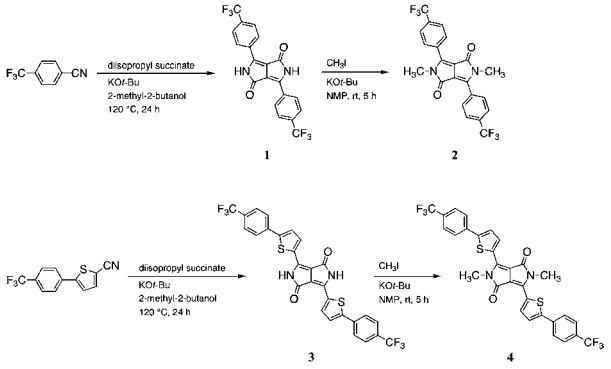

Scheme 1. Synthesis of DPP derivatives.

Table 1. Summary of photophysical properties of DPP derivatives

Compound	Solution[a]		Film	E_g^{opt}[b]/eV	
	λ_{abs}/nm	λ_{em}/nm	λ_{abs}/nm	Solution	Film
1	514, 479	530, 566	538, 494	2.31	2.07
2	486	546	502	2.53	2.15
3	582, 540	598, 652	514, 609	2.03	1.75
4	596, 554	622, 672	533, 640	2.00	1.65

[a]Obtained in 1×10^{-5} M THF solution. [b]Determined from the onset of electronic absorption wavelength: $E_g^{opt} = 1240/\lambda$ (nm).

The photophysical and electrochemical properties of DPPs are summarized in Table 1. The UV–vis spectrum of **1** in the film is red-shifted compared with that in solution due to the strong intermolecular π–π interaction and hydrogen bonding. In the case of **2**, disappearance of vibronic structure and a large Stokes shift in its fluorescence spectrum (60 nm) (Figure S2[9]) were observed, indicating loss of the molecular planarity due to the steric interaction between the methyl group and the neighboring phenyl ring. The distortion from planarity caused by *N*-substitution reduces the overlap between the π-orbitals of

Table 2. FET characteristics of DPP derivatives[a]

Compound	T_{sub}/°C	Mobility /$cm^2\,V^{-1}\,s^{-1}$	Type	I_{on}/I_{off}	V_{th}/V
1	rt	9.2×10^{-3}	n	8×10^3	18
	100	2.9×10^{-2}	n	4×10^2	16
2	rt	3.7×10^{-6}	n	20	23
3	rt	6.9×10^{-5}	n	4×10^4	43
	100	7.9×10^{-3}	n	5×10^4	37
4	rt	1.4×10^{-4}	n	20	37
		9.6×10^{-6}	p	7	−36
	100	9.3×10^{-4}	n	5	34
		1.3×10^{-5}	p	2	−45

[a]Deposition temperature (T_{sub}), field-effect mobility, current on/off ratio (I_{on}/I_{off}), and threshold voltage (V_{th}) for vapor-deposited films of DPP derivatives on HMDS-treated SiO_2.

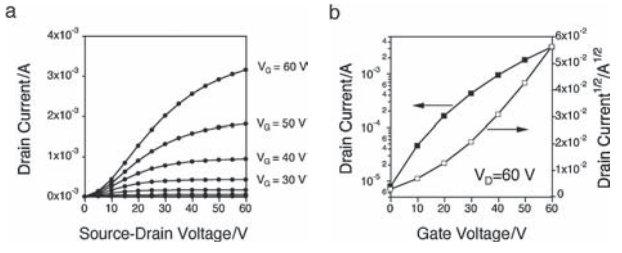

Figure 1. Output characteristic curves (a) and transfer characteristic curves (b) for FET **1** vapor-deposited on HMDS-treated SiO_2 substrates at $T_{sub} = 100\,°C$.

DPP core.[8] The UV–vis spectra of **3** and **4** are red-shifted compared with those of **1** and **2** in solution due to the extended π-conjugation and the donor–acceptor interaction. The relatively small Stokes shift in fluorescence spectrum of **4** indicates that the steric interaction between the methyl group and the neighboring thiophene ring is small and consequently distortion of the compound is insignificant. The absorption onset wavelength of the **4** film in which no intermolecular hydrogen bonding exist is longer than that of the **3** film. This suggests that the donor–acceptor interaction is stronger than the hydrogen bonding within the molecules. Cyclic voltammograms of **1** and **2** show the first reduction peaks at −0.83 and −0.86 V (vs. SCE), respectively (Figure S4[9]). The LUMO levels estimated from the first reduction potentials are low enough for efficient electron injection into the semiconductors. CV measurements could not be performed on **3** and **4** due to their low solubility. The calculated LUMO levels of them are −3.50 and −3.40 eV, respectively (Figure S9[9]). These values are slightly lower than those of **1** and **2**.

The field-effect mobilities measured on a bottom-contact/bottom-gate (BC/BG) configuration device under vacuum are shown in Table 2. The highest electron mobility of $2.9 \times 10^{-2}\,cm^2\,V^{-1}\,s^{-1}$ was obtained in **1** deposited at $T_{sub} = 100\,°C$ (Figure 1). The mobility decreased by four orders of magnitude in the film of **2** in which no hydrogen-bonding network was formed. DPP **3** with thiophene units also exhibited good electron mobilities up to $7.9 \times 10^{-3}\,cm^2\,V^{-1}\,s^{-1}$. In *N*-methyl derivative **4**, ambipolar behavior with a moderate hole mobility (up to $1.3 \times 10^{-5}\,cm^2\,V^{-1}\,s^{-1}$) was observed while the electron mobility decreased one order of magnitude. Generally, field-effect mobilities are expected to increase on the top-contact/bottom-gate (TC/BG) configuration device compared with the BC/BG device. Nevertheless, the electron mobility of **1** measured on a TC/BG configuration device was $2.0 \times 10^{-2}\,cm^2\,V^{-1}\,s^{-1}$ which is almost the same as that on the BT/BG configuration device.

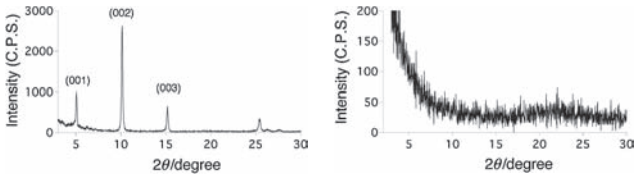

Figure 2. X-ray diffractograms of film **1** (left) and **2** (right) vapor-deposited on HMDS-treated SiO_2 at $T_{sub} = 100\,°C$.

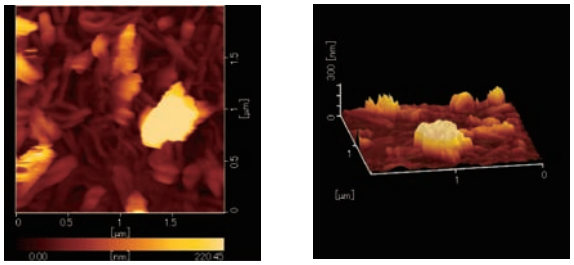

Figure 3. Surface morphology of film of **1** deposited onto HMDS-treated Si/SiO_2 at $T_{sub} = 100\,°C$.

The films of DPP derivatives deposited on SiO_2/Si substrates were investigated by X-ray diffraction in a reflection mode. Sharp reflections up to the third order were observed on the film of **1** (Figure 2), indicating formation of lamellar ordering and high crystallinity of **1** on the substrate. The *d*-spacing obtained from the first reflection peak ($2\theta = 5.06°$) is 17.5 Å. Since the molecular length of **1** obtained from the calculations is 16.2 Å, this molecule is thought to be almost perpendicular to the substrate. This is an ideal molecular arrangement for charge transport in most bottom-gate OFET configurations. No clear peak was observed on the film of **2** due to its low crystallinity (Figure 2).

As shown in AFM images of film **1** (Figure 3), large grains grew in the film. The height of grains reaches approximately 200 nm and the surface of the film is very rough. This roughness would disturb the contact between the active layer and the electrode in the TC/BG configuration device, which may be the reason for no improved electron mobility.

In summary, we have synthesized DPP derivatives possessing CF_3Ph groups with low LUMO energies and demonstrated that they act as n-type materials on FETs with a good mobility up to $2.9 \times 10^{-2}\,cm^2\,V^{-1}\,s^{-1}$. The hydrogen-bonding network leads to high crystallinity and well-ordered films, resulting in good electron transporting behavior. This suggests that incorporating hydrogen-bonding networks is valid to create high-performance n-type materials.

References and Notes

1 E. J. Meijer, D. M. de Leeuw, S. Setayesh, E. van Veenendaal, B.-H. Huisman, P. W. M. Blom, J. C. Hummelen, U. Scherf, T. M. Klapwijk, *Nat. Mater.* **2003**, *2*,

678.
2 O. Wallquist, R. Lenz, *Macromol. Symp.* **2002**, *187*, 617.
3 a) J. Mei, K. R. Graham, R. Stalder, S. P. Tiwari, H. Cheun, J. Shim, M. Yoshio, C. Nuckolls, B. Kippelen, R. K. Castellano, J. R. Reynolds, *Chem. Mater.* **2011**, *23*, 2285. b) P. Sonar, G.-M. Ng, T. T. Lin, A. Dodabalapur, Z.-K. Chen, *J. Mater. Chem.* **2010**, *20*, 3626. c) B. Walker, A. B. Tamayo, X.-D. Dang, P. Zalar, J. H. Seo, A. Garcia, M. Tantiwiwat, T.-Q. Nguyen, *Adv. Funct. Mater.* **2009**, *19*, 3063. d) A. B. Tamayo, X.-D. Dang, B. Walker, J. Seo, T. Kent, T.-Q. Nguyen, *Appl. Phys. Lett.* **2009**, *94*, 103301. e) M. Tantiwiwat, A. Tamayo, N. Luu, X.-D. Dang, T.-Q. Nguyen, *J. Phys. Chem. C* **2008**, *112*, 17402.
4 a) S.-L. Suraru, U. Zschieschang, H. Klauk, F. Würthner, *Chem. Commun.* **2011**, *47*, 1767. b) H. Yanagisawa, J. Mizuguchi, S. Aramaki, Y. Sakai, *Jpn. J. Appl. Phys.* **2008**, *47*, 4728.
5 a) Q. Tang, Z. Liang, J. Liu, J. Xu, Q. Miao, *Chem. Commun.* **2010**, *46*, 2977. b) M. Gsänger, J. H. Oh, M. Könemann, H. W. Höffken, A.-M. Krause, Z. Bao, F. Würthner, *Angew. Chem., Int. Ed.* **2010**, *49*, 740.
6 a) S. Ando, J. Nishida, E. Fujiwara, H. Tada, Y. Inoue, S. Tokito, Y. Yamashita, *Chem. Mater.* **2005**, *17*, 1261. b) S. Ando, J. Nishida, H. Tada, Y. Inoue, S. Tokito, Y. Yamashita, *J. Am. Chem. Soc.* **2005**, *127*, 5336. c) S. Ando, R. Murakami, J. Nishida, H. Tada, Y. Inoue, S. Tokito, Y. Yamashita, *J. Am. Chem. Soc.* **2005**, *127*, 14996. d) D. Kumaki, S. Ando, S. Shimono, Y. Yamashita, T. Umeda, S. Tokito, *Appl. Phys. Lett.* **2007**, *90*, 053506. e) T. Kono, D. Kumaki, J. Nishida, T. Sakanoue, M. Kakita, H. Tada, S. Tokito, Y. Yamashita, *Chem. Mater.* **2007**, *19*, 1218. f) T. Kono, D. Kumaki, J. Nishida, S. Tokito, Y. Yamashita, *Chem. Commun.* **2010**, *46*, 3265. g) K. Takimiya, Y. Kunugi, H. Ebata, T. Otsubo, *Chem. Lett.* **2006**, *35*, 1200. h) H. Wang, Y. Wen, X. Yang, Y. Wang, W. Zhou, S. Zhang, X. Zhan, Y. Liu, Z. Shuai, D. Zhu, *ACS Appl. Mater. Interfaces* **2009**, *1*, 1122.
7 a) J. Mizuguchi, *J. Phys. Chem. A* **2000**, *104*, 1817. b) J. Mizuguchi, A. Grubenmann, G. Rihs, *Acta Crystallogr., Sect. B* **1993**, *49*, 1056. c) J. Mizuguchi, A. Grubenmann, G. Wooden, G. Rihs, *Acta Crystallogr., Sect. B* **1992**, *48*, 696.
8 a) M. Vala, J. Vyňuchal, P. Toman, M. Weiter, S. Luňák, Jr., *Dyes Pigm.* **2010**, *84*, 176. b) M. Vala, M. Weiter, J. Vyňuchal, P. Toman, S. Luňák, Jr., *J. Fluoresc.* **2008**, *18*, 1181.
9 Supporting Information is available electronically on the CSJ-Journal Web site, http://www.csj.jp/journals/chem-lett/index.html.

